Steffen Matthias*, Jochen Schlobohm, Markus Kästner, and Eduard Reithmeier

Fringe projection profilometry using rigid and flexible endoscopes

Streifenprojektion mittels starrer und flexibler Endoskopie

DOI 10.1515/teme-2016-0054
Received November 11, 2016; revised December 8, 2016; accepted December 11, 2016

Abstract: Quality control is an important aspect of modern production processes. Obtaining quantitative information not only helps to ensure the function of machinery and products, but also enables cost reduction by feedback control of process parameters. A multitude of modern industrial applications feature an increasing amount of highly integrated machinery, resulting in a requirement for new measuring devices. Two new measuring systems are presented for in-situ inspection tasks in confined spaces. A combination of endoscopy techniques with structured illumination enables capturing areal 3-D geometry information of functional elements in integrated machinery. Depending on the requirements for inspection, either rigid or flexible image guides may be used to transport the structured light patterns. While a flexible endoscope allows for a more flexible positioning of the sensor head, its resolution is limited by the number of individual fiber cores. Alternatively, if constraints on the versatility of sensor positioning can be accepted, rigid endoscopes feature higher image quality. Both approaches are described in detail and compared based on evaluations on features of a calibrated micro contour standard.

Keywords: Fringe projection, 3-D metrology, endoscopy, inspection.

Zusammenfassung: Durch die Gewährleistung der Funktion von Produkten und Maschinen ist die Qualitätskontrolle ein zentrales Element moderner Produktionsketten. Die Erfassung von Qualitätskenngrößen in hochintegrierten Maschinen stellt neue Herausforderungen an die Messtechnik. Dieser Beitrag stellt zwei neu entwickelte Messsysteme vor, welche für Mess- und Prüfaufgaben an schwer zugänglichen Geometrien geeignet sind. Das erste Messsystem verwendet flexible Glasfaserbündel für den Transport der Bildinformation für Projektor und Detektor und ermöglicht so eine flexible Positionierung des Messkopfes. Das zweite Messsystem verwendet ein starres Boroskop auf Basis eines Linsensystems in Kombination mit einer Mikrokamera. Der Aufbau beider Systeme wird im Detail vorgestellt und die jeweiligen Kalibrieransätze beschrieben. Des weiteren wird ein Vergleich anhand von Wiederholmessungen an zwei Konturnormalen mit definierten Geometrieelementen durchgeführt. Die Standardabweichung der Punktedaten zu den eingepassten Referenzkörpern liegt für das auf flexiblen Bildleitern basierende System unterhalb von 5 µm sowie unterhalb von 28 µm für das starrendoskopische System. Während sich das erste Messsystem insbesondere für filigrane Verzahnungsgeometrien eignet, bietet sich die Verwendung des starrendoskopischen Systems für die Erfassung großflächiger Elemente aufgrund des größeren Messvolumens an.

Schlüsselwörter: Streifenprojektion, 3-D Messtechnik, Endoskopie, Inspektion.

***Corresponding author: Steffen Matthias,** Leibniz Universität Hannover, Institute of Measurement and Automatic Control, Nienburger Str. 17, 30167 Hannover, Germany,
e-mail: steffen.matthias@imr.uni-hannover.de.
http://orcid.org/0000-0002-6479-9742
Jochen Schlobohm, Markus Kästner, Eduard Reithmeier: Leibniz Universität Hannover, Institute of Measurement and Automatic Control, Nienburger Str. 17, 30167 Hannover, Germany

1 Introduction

In many applications highly integrated machinery is employed in order to improve efficiency and reduce costs. Examples for these applications are metal forming processes for manufacturing parts with filigree functional elements, such as gearings, or turbo jet engines for aircrafts. With an increasing use of integrated machinery, there is also a need for applicable measuring devices in order to perform quantitative inspection of functional parts. To keep the time and cost of inspection low, in-situ testing of the corresponding elements is desired, as a compllete disassembly of the machine can be avoided.

Owing to space constraints, commercially available measuring devices are not capable of performing these inspection tasks. As a result from the new requirements imposed by industrial processes, such as the sheet-bulk metal forming process [1] or the servicing of turbo jet engines [2], new measuring devices are being researched for these applications. Optical methods are capable of the task due to their fast and non-destructive nature. Especially fringe projection profilometry appears to be well-suited for the requirements thanks to its ability of capturing high-density 3-D point clouds in less than 10 s. By combining fringe projection with endoscopy techniques, known from medical applications and manual inspection of industrial machinery, quantitative information on functional elements in constrained spaces can be achieved while maintaining low measuring durations. This is especially beneficial for the inspection of production processes, where cycle times are in the order of a few seconds.

To obtain 3-D measuring data using fringe projection, structured light patterns are projected onto a specimen and received from an angle by a camera unit. Based on the deformation of the pattern in the camera images surface points can be reconstructed by triangulation. Based on different endoscopic techniques two fringe projection systems for different applications are developed and studied. For the inspection of turbine blades, a measuring system based on rigid borescopes is being developed, whereas a second measurement system based on flexible fiber endoscopes is developed for the inspection of tool geometries in an industrial metal forming process. The two endoscopy techniques differ in resolution and contrast imaging, as well as in flexibility. In this article, first common endoscopy techniques are presented and discussed followed by the description of two 3-D measuring systems based on fringe projection profilometry. Both the design and measuring procedure is described, followed by a comparison based on measurements of calibrated geometry standards.

2 Endoscopy techniques

Endoscopes are widely used for imaging tasks in medical applications and for manual inspection in industrial applications. This section gives an overview over three different techniques available for imaging applications.

Rigid endoscopes

Rigid endoscopes consist of a metal shaft containing a lens system to relay the image data. For manual inspection, they feature an ocular on one end and an objective lens on the tip. For more convenient use, a camera sensor may be attached to the endoscope to evaluate the image on a screen [3]. Rigid endoscopes are available in varying length, up to 1.5 m, with diameters of approximately 7 mm.

Fiber endoscopes

By combining multiple glass fiber cores in a common cladding to a fiber bundle, spatial image information can be transported. Current fiber endoscopes consist of up to 100 000 individual fiber cores. However, it needs to be noted that an increase in resolution also leads to a loss in flexibility, due to restrictions on the bending radius. Typically fiber endoscopes feature a diameter of less than 2 mm to also access very narrow areas with lengths of more than 1.5 m. To maintain compact dimensions at the tip, fiber endoscopes are typically combined with gradient-index (GRIN) rod lenses, which can be directly glued to the planar end surface of the bundles. By combining the fiber endoscopes with an ocular on one side, manual inspection can be achieved. Alternatively, a camera sensor may be attached.

Video endoscopes

With recent miniaturization of camera sensors, video endoscopes with an electronic camera sensor at the tip have been established. Video endoscopes are generally flexible through the use of wires for image transport and power supply. Current compact video endoscopes for medical purposes feature a resolution of more than 1 000 000 pixels [4]. The fiber-optic fringe projection system described in Section 3 uses two fiber endoscopes, while the system described in Section 4 uses a combination of a rigid endoscope and a video endoscope.

Research has been published on the development of 3-D measuring techniques for endoscopes. In [5], a measuring endoscope based on a rigid stereo endoscope has been developed, which allows to measure the distance of multiple discrete points. As an alternative to triangulation based methods, the time-of-flight method has been demonstrated using a rigid endoscope [6]. An overview over different approaches for capturing 3-D information for medical applications is presented in [7].

3 Fiber-optic fringe projection

For the inspection of tool geometries in sheet-bulk metal forming processes, a fringe projection system based on flexible fiber bundles is being developed. The system has

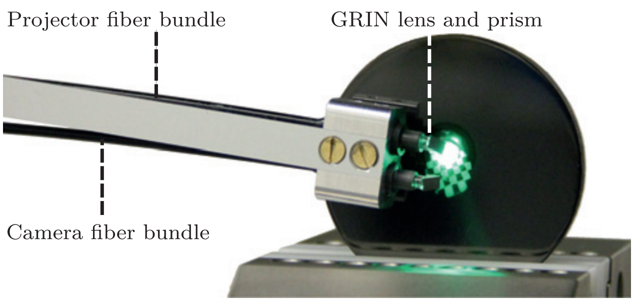

Figure 1: Fiber-optic sensor head next to specimen.

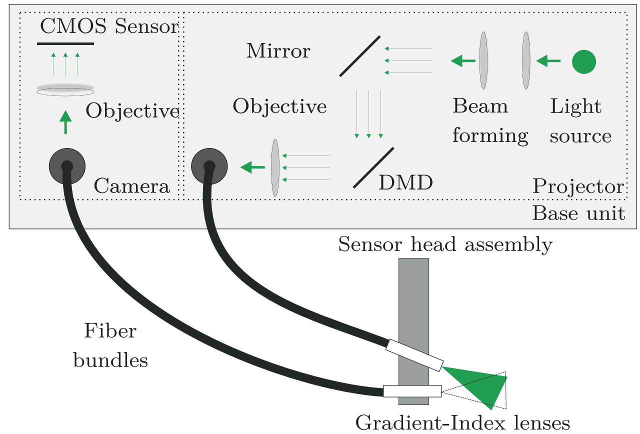

Figure 2: Schematic of the fiber-optic fringe projection system.

been designed for measurements in harsh conditions, such as increased temperatures and the presence of strong electromagnetic fields from the actuators of the forming machine. By using the fiber-bundles, sensor heads adapted to specific inspection tasks can be changed easily by removing and attaching them to the fiber ends. Design parameters for the sensor heads are the triangulation base and angle, the working distance of the optics and the use of mirror prisms to change the direction of projection. An exemplary sensor head with 10 mm working distance and mirror prisms is shown in Figure 1.

The following sections will explain the optical design of the fiber-optic fringe projection system as well as the automated calibration process and measuring algorithms developed specifically for the new system.

3.1 Optical design

The basic setup of the fringe projection system consists of a base unit and a compact sensor head, which are connected by the high resolution image fibers, as shown in the schematic in Figure 2. The fiber bundles are supplied by Fujikura Ltd. (Tokyo, Japan) and feature a resolution of 100 000 pixel at a diameter of 1.7 mm and length of 1000 mm. Figure 2 shows the basic setup of the fiber-optic system. For projecting the fringe patterns on the specimen, the sensor head features gradient-index (GRIN) lenses by GRINTECH GmbH (Jena, Germany) for both the camera and the projector part. Depending on the geometry of the object, lenses with a working distance of 10 mm or 20 mm may be used. Optionally mirror prims may be used to change the direction of projection by 90°. Using the 10 mm GRIN lenses, the measuring volume is approximately $6 \times 6 \times 3\ \text{mm}^3$. For the lenses with a working distance of 20 mm, the measuring volume is approximately $10 \times 10 \times 4\ \text{mm}^3$. For the measurements presented in Section 5, a sensor head with a working distance of 10 mm has been used.

Depending on the requirements defined for the inspection task, either a Laser light source or a LED may be used in the pattern projector. While the Laser light source enables very efficient fiber coupling and thus very low measuring durations, it suffers from slightly increased noise in the 3-D point cloud data. Alternatively, a LED-based illumination may be used to avoid speckle [8], with measuring durations in the range of 3 s and less, depending on the reflectance of the specimen. For the measurements presented in this article, an LED light source is used in the pattern generator. After a beam shaping stage, a digital micro-mirror device (DMD) by Texas Instruments Incorporated (Dallas, USA) with a resolution of 1024×768 pixels is used for the flexible generation of fringe patterns. In order to couple the generated patterns to the fiber bundle, a microscopy objective is used.

On the camera side, a Point Grey GS3-U3-23S6M-C industrial camera (FLIR Integrated Imaging Solutions GmbH, Ludwigsburg, Germany) with a CMOS sensor is used to capture phase-shift images. Outcoupling from the fiber bundle is achieved by using a microscopy objective.

3.2 Calibration and measuring process

The measurement process for the fiber-optic fringe projection system is based on phase-shift patterns. To avoid artifacts from low-frequency inter-fiber crosstalk, heterodyne phase unwrapping is used in combination with deconvolution of the modeled fiber bundle point spread function [9]. As technical surface geometries exhibit highly varying reflectivity, high dynamic range (HDR) imaging is used during the phase measuring process. After obtaining a phase-image of the specimen, a high-density point cloud can be reconstructed by triangulation using calibration data for the chosen system model.

In order to calibrate the fiber-optic fringe projection system, a diffuse reflective point pattern standard by Edmund Optics GmbH (Karlsruhe, Germany) is positioned by a linear stage. The standard features a grid of defined points with a distance of 125 µm. To capture the required calibration data, the standard is automatically positioned at different distances to the sensor head. An automated algorithm is used to extract projector and camera correspondences from the captured calibration images. In a third step, the system model parameters are calculated from the correspondences. Depending on the optics used in the projector, two different calibration models are employed. For the GRIN rod lenses with parallel end planes, distortion can be very effectively described by radial distortion polynomials of third order according to the Brown distortion model [10]. When considering the full optical path, including incoupling and outcoupling objectives, tangential distortion coefficients can also be estimated by the calibration algorithm. If a GRIN lens with angled end plane is used in the projector path, asymmetric distortions are present in the projected images. In this case, a polynomial black-box model can be used for the projector instead of the pinhole model.

The calibration process and a comparison of the two different system models is described in detail in [11].

4 Borescopic fringe projection

For the measurement of complex shaped goods, a borecopic fringe projection system was developed. As shown in Figure 3, it consists of a compact LED Beamer (TI LCR4500), an optical adapter, a rigid Borescope from *Storz* and a 5 mega pixel chip-on-tip camera (OmniVision OV5647). Figure 4 shows the measurement tip with a diameter of approximately 7 mm. The projector is a development system. It can project 120 greyscale images per second with a resolution of 912 × 1140 pixel. The camera is driven by a compact single-board computer and the images are send to the measurement computer via fast-ethernet. Although the camera has a color CMOS sensor, only greyscale information is used for calibration and measurement. The borescope has an angle of view of 90° and is pointed 70° relative to the shaft. The camera has an angle of 60° and is pointed 90° relative to the shaft. The triangulation angle is 20°. At a distance of 30 mm the the field of view is approximately 20 mm × 30 mm.

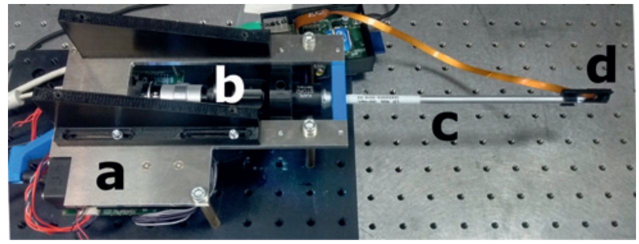

Figure 3: Photograph of the measurement system with the projector (a), optical lens (b), borescope (c), micro-camera (d).

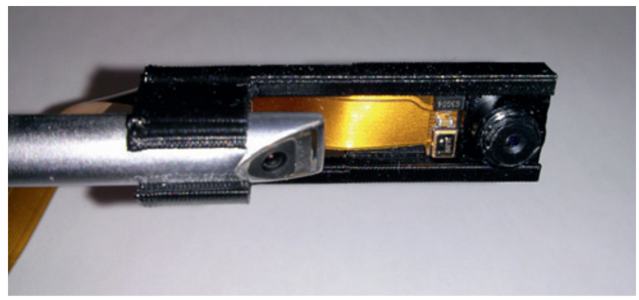

Figure 4: Photograph of the chip-on-tip camera (7 mm wide).

4.1 Calibration

The calibration follows the method from Zhang [12] adopted for fringe projection systems by Pösch [13]. The camera and the projector are both modelled as cameras with a camera matrix and distortion coefficients each. A calibration pattern with yellow dots is positioned in front of the measurement system. First the projector projects blue light onto the pattern that results in the yellow features being visible as dark features in the camera image. Afterwards the projector projects dark features with a yellow background onto the calibration plane. Now the yellow printed features are barely visible and only the projected features are visible in the camera image. Additionally the projected pattern contains several rings to identify the features position on the projectors display. This procedure is repeated several times with the calibration plane each time in a different pose. For each plane position a homography between the camera and the projector is estimated. With one homography for each plane position, the relative pose of the camera and the projector and both systems' internal parameters can be calculated e.g. using OpenCV [14]. Figure 5 shows example calibration images.

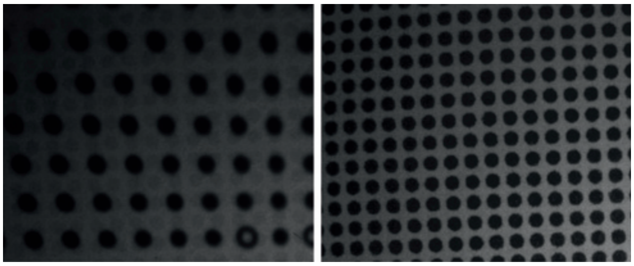

Figure 5: Two calibration images. The camera first took a picture of yellow features with blue light from the projector (left). Afterwards the projector projected dark features with yellow background so that the printed features are barely visible (right).

Table 1: Step feature (calibration certificate: 1000.5 μm ± 0.4 um, $k = 2$).

	Fiberscope	Borescope
Mean	1002.0 μm	987.3 μm
Standard deviation	0.1 μm	1.6 μm
Point-reference SD	4.3 μm	27.9 μm

Table 2: Radius feature (calibration certificate: 1001.5 μm ± 0.7 um, $k = 2$).

	Fiberscope	Borescope
Mean	1003.0 μm	924.6 μm
Standard deviation	0.1 μm	1.0 μm
Point-reference SD	2.5 μm	20.8 μm

Table 3: Radius feature (calibration certificate: 5994.0 μm ± 1.2 um, $k = 2$).

	Fiberscope	Borescope
Mean	5968.3 μm	5954.1 μm
Standard deviation	1.2 μm	1.3 μm
Point-reference SD	3.5 μm	20.1 μm

5 Measurement results

In order to evaluate the performance of both fringe projection systems, two calibrated micro contour standards are measured. The first standard (IF-Verification Tool) has been developed by Alicona Imaging GmbH (Graz, Austria) in cooperation with the German national metrology institute PTB. Additionally, a contour standard for the tactile measuring device Hommel-Etamic T8000 by Jenoptik AG (Jena, Germany) with larger features is measured.

On the smaller micro-contour standard a cylindrical feature with a radius of 1 mm and a step feature with a height of 1 mm is measured using both measuring devices. Additionally, the cylindrical feature with a radius of 6 mm is measured on the larger contour standard.

According to the evaluation type A of the Guide to the Expression of Uncertainty (GUM) [15], 25 measurements for each geometry feature are obtained, while the pose of the sensor is kept constant.

In addition to the evaluation of feature parameters, also the standard deviation (SD) of the measured point distance to the best-fit reference surface is calculated. For the step feature, a plane is fitted to the upper step surface and the average distance of the points on the lower step surface to the fitted plane is calculated in order to obtain the measured step height.

Both devices achieve accurate measurements of the geometry features, with a deviation of the measured radii and step heights of less than 26 μm for the fiber-optic system and less than 77 μm for the borescopic system compared to the calibrated values. As seen in Tables 1 and 2, the deviation is also significantly lower for the smaller elements for the fiber-optic system as they are a better fit for the measuring volume. For the larger radius feature shown in Table 3, the standard deviation is increased with a value of 1.2 μm compared to 0.1 μm for the smaller radius for the fiber-optic system. The standard deviation of the individual measured points to the fitted reference surface are approximately 8 μm for the fiber-optic system and around 21 μm for the borescopic system.

6 Discussion

The measurements presented in Section 5 show only slight deviations to the calibrated reference values of the features. Especially the strong aberrations of the projector and camera optics of both systems are successfully compensated for by the calibration strategies. Owing to the smaller field of view, the fiber-optic fringe projection system is capable of measuring the cylindrical feature with a radius of 1 mm and the step feature with 1 mm height with a lower standard deviation compared to the borescopic fringe projection system. When evaluating the larger cylindrical feature with a radius of 6 mm, the repeatability of the measurements obtained with the borescopic system is improved in comparison with the fiber-optic system as a result of the size of its measuring volume. The measurements demonstrate the capability of both systems for the inspection of machine parts in constrained spaces. The fiber-optic fringe projection system is especially suited for the inspection of gearing geometries on metal forming tools, with radii in the range of 2 mm or less, while the borescopic system is useful for the inspection of larger turbine blade surface areas.

7 Summary

Two measuring devices for the inspection of occluded geometries have been presented. By combining fringe projection and endoscopy techniques, the systems are applicable for measurements of geometries in hard-to-reach spaces. The optical design and calibration approaches for a fringe projection system based on high-resolution fiber bundles and a fringe projection system based on a rigid endoscope and a miniature camera have been described.

Both systems have been compared on the basis of evaluations of measurements of two calibrated geometry standards. Using the fiber-optic fringe projection system, measurements of cylindrical and step geometries with a standard deviation of less than 10 μm are achieved. Alternatively, the borescopic fringe projection system allows for the inspection of larger areas in a single measurement.

Acknowledgement: The authors would like to thank the German Research Foundation (DFG) for funding the projects within the collaborative research centers SFB/TR 73 and SFB 871.

References

1. M. Merklein, J. M. Allwood, B.-A. Behrens, A. Brosius, H. Hagenah, K. Kuzman, K. Mori, A. E. Tekkaya, A. Weckenmann. Bulk forming of sheet metal. In *Annals of the CIRP*, volume 61, pages 725–745, 2012.
2. B. Denkena, V. Boess, D. Nespor, F. Floeter, F. Rust. Engine blade regeneration: A literature review on common technologies in terms of machining. *The International Journal of Advanced Manufacturing Technology*, 81(5–8):917–924, 2015.
3. G. Berci, J. Davids. Endoscopy and television. *British medical journal*, 1(5292):1610, 1962.
4. Y. M. Bhat, B. K. Abu Dayyeh, S. S. Chauhan, K. T. Gottlieb, J. H. Hwang, S. Komanduri, V. Konda, S. K. Lo, M. A. Manfredi, J. T. Maple. High-definition and high-magnification endoscopes. *Gastrointestinal Endoscopy*, 80(6):919–927, 2014.
5. M. Chan, W. Lin, C. Zhou, J. Y. Qu. Miniaturized three-dimensional endoscopic imaging system based on active stereovision. *Applied Optics*, 42(10):1888, 2003.
6. J. Penne, K. Höller, M. Stürmer, T. Schrauder, A. Schneider, R. Engelbrecht, H. Feußner, B. Schmauss, J. Hornegger. Time-of-flight 3-d endoscopy. In *Medical Image Computing and Computer-Assisted Intervention–MICCAI 2009*, pages 467–474. Springer, 2009.
7. J. Geng, J. Xie. Review of 3-d endoscopic surface imaging techniques. *IEEE Sensors Journal*, 14(4):945–960, 2014.
8. S. Matthias, M. Kästner, E. Reithmeier. Comparison of laser and led illumination for fiber-optic fringe projection. In Francis Berghmans and Anna G. Mignani, editors, *SPIE Photonics Europe*, SPIE Proceedings, page 989905. SPIE, 2016.
9. S. Matthias, M. Kästner, E. Reithmeier. Modeling of imaging fiber bundles and adapted signal processing for fringe projection. *Advanced Optical Technologies*, DOI: https://doi.org/10.1515/aot-2016-0050, 2016.
10. D. C. Brown. Decentering distortion of lenses. *Photometric Engineering*, 32(3):444–462, 1966.
11. S. Matthias, M. Kästner, E. Reithmeier. Evaluation of system models for an endoscopic fringe projection system. *Measurement*, 73:239–246, 2015.
12. Z. Zhang. A flexible new technique for camera calibration. *Pattern Analysis and Machine Intelligence, IEEE Transactions on*, 22(11):1330–1334, 2000.
13. A. Pösch. *Fast detection and Analysis of Geometry Defects on Free Form Surfaces Using Model-Based Inverse Fringe Projection*. PhD thesis, Leibniz Universität Hannover, 01.01.2014.
14. Opencv (http://opencv.org).
15. Bureau International Poids et Des Mesures, Commission électrotechnique internationale, and Organisation internationale de normalisation. *Guide to the Expression of Uncertainty in Measurement*. International Organization for Standardization, 1995.

Bionotes

Steffen Matthias
Leibniz Universität Hannover, Institute of Measurement and Automatic Control, Nienburger Str. 17, 30167 Hannover, Germany
steffen.matthias@imr.uni-hannover.de

Steffen Matthias is a research associate at the Institute of Measurement and Automatic Control at Leibniz Universität Hannover.

Jochen Schlobohm
Leibniz Universität Hannover, Institute of Measurement and Automatic Control, Nienburger Str. 17, 30167 Hannover, Germany
jochen.schlobohm@imr.uni-hannover.de

Jochen Schlobohm is a research associate at the Institute of Measurement and Automatic Control at Leibniz Universität Hannover.

Markus Kästner
Leibniz Universität Hannover, Institute of Measurement and Automatic Control, Nienburger Str. 17, 30167 Hannover, Germany
markus.kaestner@imr.uni-hannover.de

Markus Kästner is the head of the department for production metrology at the Institute of Measurement and Automatic Control at Leibniz Universität Hannover.

Eduard Reithmeier
Leibniz Universität Hannover, Institute of Measurement and Automatic Control, Nienburger Str. 17, 30167 Hannover, Germany
sekretariat@imr.uni-hannover.de

Eduard Reithmeier is the head of the Institute of Measurement and Automatic Control at Leibniz Universität Hannover.